Colloids and Surfaces A: Physicochem. Eng. Aspects 388 (2011) 21–28

Contents lists available at ScienceDirect

Colloids and Surfaces A: Physicochemical and Engineering Aspects

journal homepage: www.elsevier.com/locate/colsurfa

Role of polycation adsorption in poly-Si, SiO_2 and Si_3N_4 removal during chemical mechanical polishing: Effect of polishing pad surface chemistry

Naresh K. Penta, John B. Matovu, P.R. Dandu Veera [1], Sitaraman Krishnan, S.V. Babu *

Department of Chemical and Bio-molecular Engineering, and Center for Advanced Materials Processing, Clarkson University, Potsdam, NY 13699, USA

ARTICLE INFO

Article history:
Received 20 June 2011
Received in revised form 22 July 2011
Accepted 28 July 2011
Available online 5 August 2011

Keywords:
CMP
Poly-Si
SiO_2
Si_3N_4
PDADMAC
Polishing pads
Bridging attraction
Eosin Y staining

ABSTRACT

The dramatic differences in the effects of two different polishing pads (IC1000 and Politex) on the removal rates (RRs) of poly-Si, SiO_2, and Si_3N_4 films during chemical mechanical polishing using aqueous abrasive-free solutions of a cationic polymer, poly(diallyldimethyl ammonium chloride) (PDADMAC), are described. For example, with a 250 ppm of aqueous PDADMAC solution, poly-Si RR is <1 nm/min with a Politex pad but is about 500 nm/min using an IC1000 pad. The difference in the RRs is attributed to differences in the strengths of PDADMAC-mediated bridging interactions between the pads and the substrates. Also, when the same 250 ppm of PDADMAC was used as an additive in either silica- or ceria-based dispersions, the RRs of both SiO_2 and Si_3N_4 films were suppressed to less than 1 nm/min for both pads. Possible mechanisms for the observed differences in the RRs of poly-Si, SiO_2, and Si_3N_4 on the two pads are discussed based on elemental analysis of the pads, X-ray photoelectron spectroscopy, and zeta potential measurements (of the pads in the absence and presence of PDADMAC). Also, the results of exposure to eosin Y, a dye that changes color on exposure to PDADMAC provided useful insights into the strength of the bridging attraction between the pads and PDADMAC.

1. Introduction

Chemical mechanical planarization/polishing (CMP), a process widely used in semiconductor manufacturing technology, utilizes several types of polishing pads which differ in their surface morphology, hardness, porosity and structure. Some of the more popular pads include Suba, Politex, and the IC-series of pads, stacked with and without Suba pads. Politex pads are made from microporous urethane having a surface morphology derived from the ends of columnar void structures in bulk urethane and are grown on a urethane felt base [1]. IC-series pads are filled and/or blown composite urethanes having surface structures made up of hemispherical depressions derived from exposed hollow spherical elements or incorporated gas bubbles [1]. The method of manufacturing provides these two pads with different intrinsic properties such as chemical composition, specific density, pore size, surface roughness, and hardness. The traditional role of such polishing pads has been to hold, disperse and rejuvenate the slurry in the pores, transmit the load to the abrasives and wafer, and assist with the planarization of the surface topography of the substrate [2]. Several studies [3] revealed distinguishable differences among these pads during CMP in slurry transportation, wafer-pad contact area, polish rates of thin films, degradation of the pad when exposed to certain chemicals, and extent of dishing caused by pad bending. Some properties of the polishing pad can also influence key process metrics such as pattern sensitivity of the polish rates, local and global across-wafer uniformity, etc. [4,5]. Other studies have also focused on the differences in pad glazing, conditioning and soaking in water, and chemical or physical modification of the pad surfaces [6,7].

In view of these differences, Politex and IC1000 pads have been used for different applications in the semiconductor industry. For example, Politex pads are widely used for removing tungsten, tantalum, and tantalum nitride and for various buffing steps, while IC1000 pads are used to produce high planarization efficiencies [8].

These pads are also used during the polishing and planarization of three dielectric films (poly-Si, SiO_2 and Si_3N_4) that are important and challenging during the fabrication of recently developed Fin Field-effect-transistor (FinFET) devices [9,10], in the replacement metal gate (RMG) technique for the fabrication of high-k/metal gate structures [11], in creating shallow trench isolation (STI) structures [10], and in the processing of microelectromechanical systems (MEMS) [12]. In this paper, we extend our recent work [13] in which aqueous solutions of a cationic polymer, poly(diallyldimethyl ammonium chloride) (PDADMAC), were shown to polish poly-Si at a rate of about 500 nm/min at pH 10 using an IC1000 pad. Here we show that removal rates (RRs) of poly-Si films are significantly

* Corresponding author.
E-mail address: babu@clarkson.edu (S.V. Babu).
[1] Currently working at Intel Corporation, Portland, Oregon, USA.

0927-7757/$ – see front matter © 2011 Elsevier B.V. All rights reserved.
doi:10.1016/j.colsurfa.2011.07.039

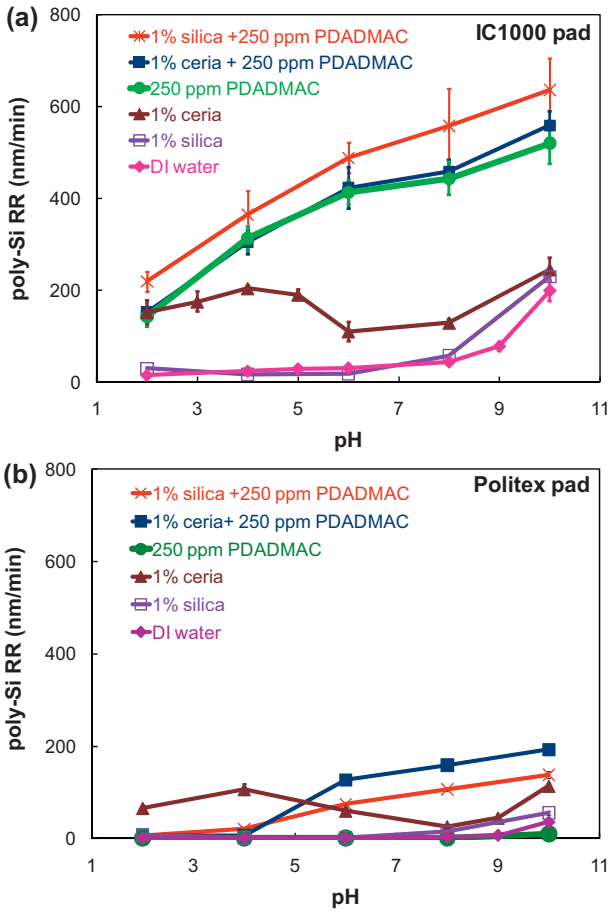

Fig. 1. RRs of poly-Si films on IC1000 pad (a) and Politex pad (b), respectively, as a function of pH using abrasive-free solutions and ceria/silica dispersions with and without 250 ppm PDADMAC. Part a is from Ref. [13].

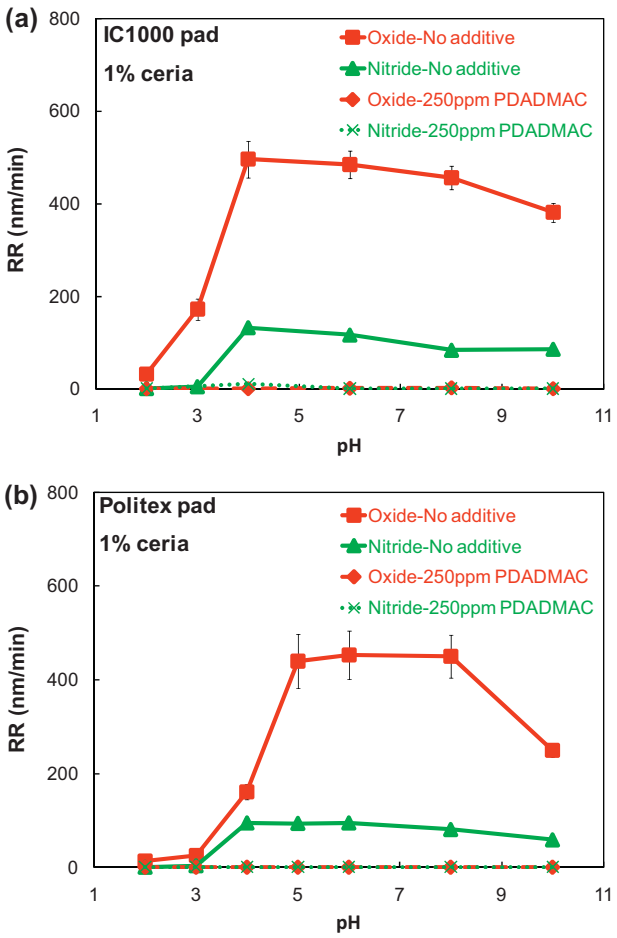

Fig. 2. RRs of both oxide and nitride films on IC1000 and Politex pad, respectively, as a function of pH using 1% ceria ($d_{mean} \sim 180$ nm) dispersions with and without 250 ppm PDADMAC. Part a is from Ref. [13].

different when the softer Politex pads are used. The RRs of poly-Si, SiO_2, and Si_3N_4 films obtained using aqueous abrasive-free solutions and ceria and silica dispersions, with and without 250 ppm PDADMAC, were reported earlier but only for an IC1000 pad [13], and are again presented (Figs. 1a, 2a and 3a) for ease of comparison with the new data reported here.

The experiments described herein show that, using 250 ppm of an abrasive-free aqueous solution of a cationic polymer, PDADMAC (MW ~ 200,000 g/mol), the RRs of poly-Si can be suppressed to <1 nm/min on a Politex pad at all pH values tested in the range of 2–10 (Fig. 1b) in sharp contrast to the RRs increasing from ~200 nm/min to ~500 nm/min as the pH is increased from 2 to 10 with the IC1000 pad (Fig. 1a) [13]. On adding either 1 wt% silica or ceria abrasives to 250 ppm of aqueous PDADMAC solutions, the poly-Si RRs on the Politex pad were enhanced somewhat, but only for pH > 4 and still considerably lower than those on an IC1000 pad, while the RRs of both the SiO_2 and Si_3N_4 films were suppressed to <1 nm/min on both the pads. In the following, these RRs are described in detail along with the results of several other measurements performed to explain them. In contrast to the results of Chen and Yen [14], who showed that the hardness of the pads and the abrasives and the electrostatic interactions affect the RRs of poly(silsesquioxane), our analysis suggests that the strength of the bridging attraction between the pad, wafer surface and PDADMAC molecules is the dominant factor in determining the RRs reported here.

2. Experimental

2.1. Materials

An aqueous dispersion of ceria abrasives ($d_{mean} \sim 180$ nm, 50 wt%) was supplied by Ferro Corp. The same dispersion was used in several of our earlier publications [15,16], and its characteristics are available there. Colloidal silica abrasives (NexSil 85A, $d_{mean} \sim 50$ nm), stabilized at pH 3.5, were supplied by Nyacol Nano Technologies. Silicon nitride particles, PDADMAC (MW ~ 200,000 g/mol), and the pH adjusting agents (KOH and HNO_3) were all obtained from Sigma–Aldrich. Eosin Y dye was purchased from Alfa Aesar. The two types of polishing pads (IC1000 K-groove and Politex) and the diamond grit conditioner used here were supplied by Dow Electronic Materials and 3M, respectively. Blanket poly-Si films (2000 nm thick, low pressure chemical vapor deposited (LPCVD) at about 610 °C on silicon wafers) were obtained from DK Nanotechnology. Thermal oxide (2000 nm thick, grown at 900 °C) and silicon nitride films (500 nm thick, LPCVD at 790 °C) grown on silicon substrates were obtained from Montco-Silicon Technologies, Inc. While the poly-Si and silicon nitride films were deposited on an intervening 100 nm thick silicon dioxide layer grown on 8 in. diameter silicon wafers, the thermal oxide was directly grown on the silicon substrate. Each of these 8 in. wafers was cut into several 2 in. diameter pieces, which were then used for polishing.

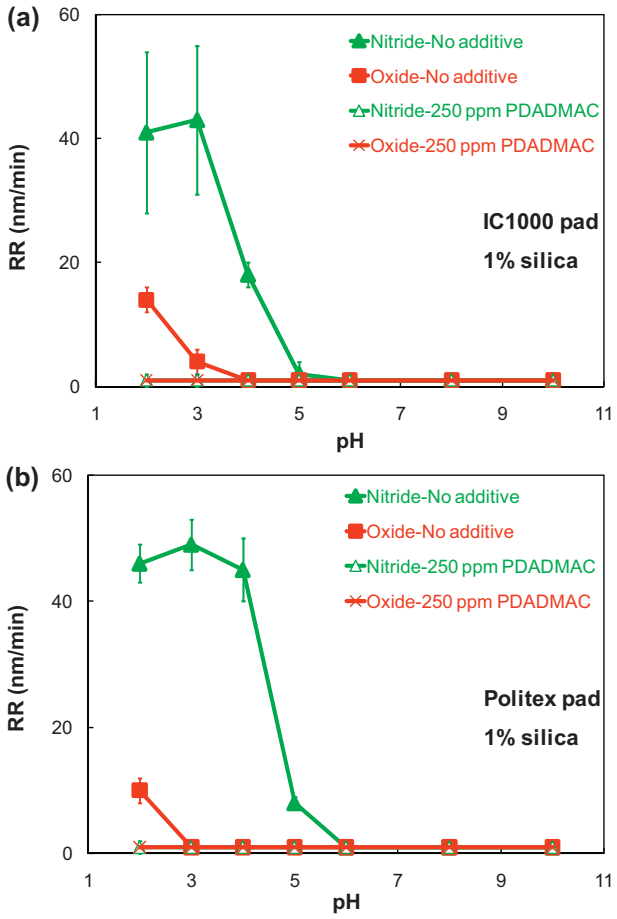

Fig. 3. RRs of both oxide and nitride films on IC1000 and Politex pad, respectively, as a function of pH using 1% silica ($d_{mean} \sim 50$ nm) dispersions with and without 250 ppm PDADMAC. Part a is from Ref. [13].

2.2. Methods

2.2.1. Determination of RRs

The 2 in. diameter wafers were polished for one minute on a CETR polisher at 4 psi down pressure, 90/90 rpm carrier/platen speed, and a slurry flow rate of 120 ml/min. The IC1000 pad (k-groove) was conditioned for one minute using a 4 in. diameter diamond-grit conditioner after each polishing but no conditioning was performed for the Politex pad. A Filmetrics interferometer was used to measure the thickness of the different films (oxide, Si_3N_4, and poly-Si) before and after polishing. The RR of each of these films was determined from the difference between pre- and post-polished film thickness values. The reported RR for each experiment is the arithmetic average of the RRs measured for two different wafers, each at 16 points located across a diameter of the wafer. The standard deviation in RRs was based on the data for these 32 points.

2.2.2. Surface characterization of polishing pads

2.2.2.1. X-ray photoelectron spectroscopy (XPS). Chemical compositions of the surfaces of a conditioned IC1000 and un-conditioned Politex pads were determined using XPS. Survey scans and high resolution C 1s XPS were acquired using Surface Science Instruments model SSX-100 spectrometer (Eastman Kodak, Rochester, NY). A monochromatic Al Kα X-ray source at 1486.6 eV was used. Photoelectrons were collected at an angle of 55° from the surface normal and analyzed using a hemispherical analyzer with a pass energy of 150 eV for survey scans and 50 eV for high resolution scans. Charge compensation was carried out using low-energy electrons from an electron flood gun. The spectra were analyzed using the CasaXPS software. These experiments were performed at Cornell Center for Materials Research.

2.2.2.2. Zeta potential measurements. A ZetaSpin 1.2 apparatus (Zetametrix, Inc., USA) was used to determine the zeta potentials of both IC1000 and Politex pad surfaces. These measurements were conducted in a 0.001 M aqueous solution of KCl, with and without the addition of PDADMAC. The zeta potentials were calculated from the streaming potentials measured in the vicinity of a rotating disk to which the polishing pad sample was attached. Ideally, samples with a flat surface are necessary for the conversion of streaming potentials to zeta potential values. Hence, a 1 in. diameter sample of the IC1000 pad was obtained from the center of the pad, where the surface texture was smooth. The surface of the Politex pad sample was smoothed using a sharp diamond-coated knife edge.

2.2.3. Bulk compositions of pads

FT-IR spectroscopy and elemental analysis of the solids collected by scraping the IC1000 and Politex pad surfaces were performed at QTI, Whitehouse, NJ. The IR spectra were acquired in the reflectance mode. C, H, and N compositions were determined using a PerkinElmer 2400 Elemental Analyzer, wherein these elements are converted to the gases, CO_2, H_2O, and N_2, respectively, by combustion in pure oxygen. Thermal conductivity measurements are then used to obtain the molar amounts of these gases. The Oxygen Accessory Kit was used to determine O in the sample, using pyrolysis to convert O to CO followed by thermal conductivity detection of CO. A colorimetric titration assay was used to determine Cl in the samples. Combustion of the sample in an oxygen combustion flask in the presence of H_2O_2 resulted in the formation of chloride, which was titrated with mercuric nitrate in the presence of phenylazoformic acid 2-phenylhydrazide.

3. Results and discussion

3.1. Polishing results

Poly-Si RRs: Fig. 1 shows the poly-Si RRs obtained on an IC1000 and a Politex pad, in the pH range of 2–10 using pH-adjusted deionized (DI) water, aqueous solutions of 250 ppm of PDADMAC, and 1 wt% ceria/silica suspensions with 250 ppm PDADMAC and without PDADMAC. A PDADMAC concentration of 250 ppm was chosen for all our experiments since the RRs of poly-Si obtained were high at this concentration [13].

The poly-Si RRs are generally lower on a Politex pad compared to the RRs with the IC1000 pad in all these cases (Fig. 1b). More significantly, with the Politex pad, no poly-Si RRs were observed using abrasive-free solutions of 250 ppm of PDADMAC in the pH range of 2–10. Adding either 1 wt% ceria or silica abrasives enhanced the RRs somewhat, especially above pH 4, but they are still much lower than those with the IC1000 pad.

SiO_2 and Si_3N_4 RRs: Unlike the poly-Si RRs, the oxide and nitride RRs on both the pads were ~0 nm/min when polished using pH-adjusted DI water as well as 250 ppm of aqueous PDADMAC solutions in the pH range of 2–10. These data are not shown.

Fig. 2 shows the RRs of the oxide and nitride films using an IC1000 pad and a Politex pad with 1 wt% ceria ($d_{mean} \sim 180$ nm) dispersions in the presence and absence of PDADMAC (250 ppm concentration). Using 1 wt% ceria with no PDADMAC and with the IC1000 pad, the oxide RR is about 10 nm/min at pH 2, about 180 nm/min at pH 3 and greater than 400 nm/min in the pH range of 4–10 while the nitride RR is less than 10 nm/min below pH 4 and about 100 nm/min in the pH range of 4–10. With the Politex pad, the sharp increase in the oxide RRs (which was observed at

pH between 3 and 4 while using the IC1000 pad) occurred at a pH between 4 and 5. In the pH range 5–8, the oxide RRs on the Politex pad are very similar to those on the IC1000 pad. However, beyond pH 8, the oxide RR decreased sharply for the Politex pad, while only a smaller decrease was observed with the IC1000 pad. The differences in the nitride RRs in the pH range of 2–10 were negligible for the two pads investigated.

Significantly, the addition of 250 ppm of PDADMAC to the ceria dispersion led to a suppression of the oxide and nitride RRs to below 1 nm/min on both the pads (Fig. 2). Before proceeding further, we would like to point out that the enhancement of poly-Si RR on the IC1000 pad using 250 ppm PDADMAC in the absence or presence of ceria or silica, and the simultaneous suppression of both the oxide and nitride RRs is very useful in the fabrication of FinFET and MEMS devices. On the other hand, the suppression of poly-Si RRs on the Politex pad using aqueous solutions of the same polymer can be useful for the RMG CMP applications provided higher oxide and/or nitride RRs can be maintained with suitable additives. Indeed, this is possible and will be discussed in a separate publication.

Fig. 3 compares the RRs of both oxide and nitride films on IC1000 and Politex pads using 1 wt% silica ($d_{mean} \sim 50$ nm) dispersions with and without 250 ppm PDADMAC. Using 1 wt% silica with no additive and IC1000 pad, the oxide RR is ~15 nm/min at pH 2 and decreased to <1 nm/min as the pH was increased above 3. A similar oxide RR trend (lower at pH 2 and 3) was observed on the Politex pad. In the case of nitride films, the RRs on the IC1000 pad are about 40 nm/min at pH 2 to 3 and then decreased above pH 3, reaching <1 nm/min for pH ≥ 5. With the Politex pad also, the same big drop in the nitride RR occurred, but now beyond pH 4 and again reaching <1 nm/min for pH ≥ 6.

Adding 250 ppm of PDADMAC to 1 wt% silica dispersions suppressed both the oxide and nitride RRs to <1 nm/min on both the pads over the entire pH range just as with ceria dispersions. Before proceeding further, it should be noted that using the Politex pad at pH 3 or 4, the 1 wt% silica based slurries without any additive produced comparatively high nitride RR (about 50 nm/min) and very low oxide and poly-Si RRs (both below 1 nm/min). Hence, this pad-slurry combination is potentially attractive for reverse STI and RMG applications when high nitride and low oxide/poly-Si RRs are required.

Chen and Yen [14] compared the relative performance of an IC1400 hard pad with a Politex soft pad on the CMP of low-k poly(silsesquioxane) films. They found that the hardness of the abrasives and the pads and the electrostatic interaction between the abrasive and polymer surface strongly affected the RRs. Our polishing results above suggest that the RRs of oxide and nitride films on the hard IC1000 pads and the soft Politex pads were relatively the same when either ceria or silica abrasives were used, except at specific pH values. Hence, the hardness of the pads or the abrasives alone cannot explain the difference in the observed dramatic drop in the poly-Si RRs. In order to examine the role of possible differences in the intermolecular forces of interactions between the pad/abrasive/substrate surfaces, the chemical composition of the pads (particularly their surface compositions) were probed in detail using FT-IR spectroscopy, elemental analysis, and X-ray photoelectron spectroscopy in these studies. The results are described below.

3.2. Infrared spectroscopy

Both pads showed a peak at 814 cm^{-1}, corresponding to the C–H deformation of the aromatic rings (from the hard segment of the polymer). For comparison of chemical composition of the two pads, the IR spectra were normalized such that the absorbances are the same for this peak. The peaks observed at 1600 cm^{-1} correspond to the C=C stretching vibrations of the aromatic rings (spectra not shown). The absorbances of these peaks were nearly the same for the two pads, as expected. The peak at 1101 cm^{-1} corresponds to the C–O stretch of the polyether soft segments in the polyurethane. The absorbance of this peak was higher in the case of the Politex pad, which is consistent with the soft nature of this pad.

The C=O stretching vibrations of the urethane groups (amide I bands) were seen at 1713 cm^{-1} in IC1000 and 1729 cm^{-1} in Politex. The peaks at 1521 cm^{-1} and 1533 cm^{-1} are also attributed to the urethane groups (amide II bands). The higher intensity of the amide II band in IC1000 indicates the presence of a large number of urethane groups in this pad (which is again in agreement with the higher hardness of IC1000).

Table 1
Surface compositions of IC1000 and Politex pads determined using XPS.

	IC1000		Politex	
	Atomic %	No. of atoms relative to C (%)	Atomic %	No. of atoms relative to C (%)
C	64.9	100	75.5	100
N	6.1	9	0.8	1
O	22.0	34	22.4	30
Cl	3.3	5	0.8	1
Si	3.7	6	0.5	<1

3.3. X-ray photoelectron spectroscopy

The surface compositions of the pads were determined using X-ray photoelectron spectroscopy, using an electron emission angle of 55°. At this angle, the XPS probe depth is estimated to be about 3.5 nm. The XPS survey scan for the IC1000 pad is shown in Fig. 4 and the compositions of different elements present at the surfaces of the two pads are summarized in Table 1. Atom compositions were calculated using the area of the peaks, Scofield photoionization cross section, and assuming 0.7th power dependence of the sampling depth on kinetic energy of photoelectrons.

The surface concentration of N in IC1000 is higher than that in Politex, evidently from a larger number of urethane (–OC(=O)NH–) and urea (–NHC(=O)NH–) linkages in the IC1000 pad, which makes it harder. The surface concentration of Cl was also found to be higher in the IC1000 pad than in Politex. This Cl could be introduced into polyurethane through the use of chlorinated polyols [18] or by treating the polyurethane with NaOCl solutions [17]. Other studies have similarly detected Cl in the IC1000 pad using XPS and EDS [19–21]. Si was detected at the surfaces of both the pads. Ramsdell et al. [19] have also found the presence of Si at the surface of IC1000. The Si could be from silica fillers intentionally added to the

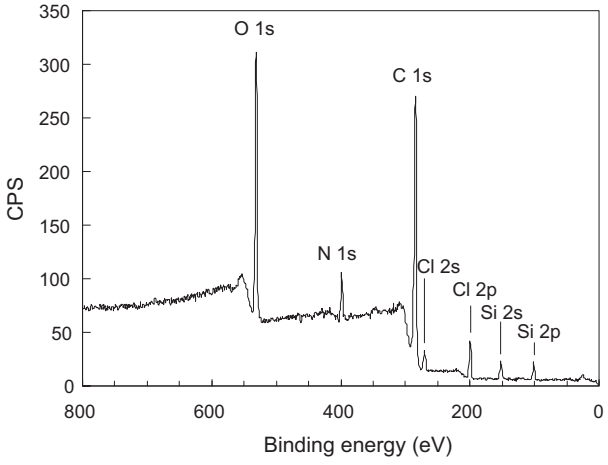

Fig. 4. XPS survey scan of the surface of the IC1000 pad.

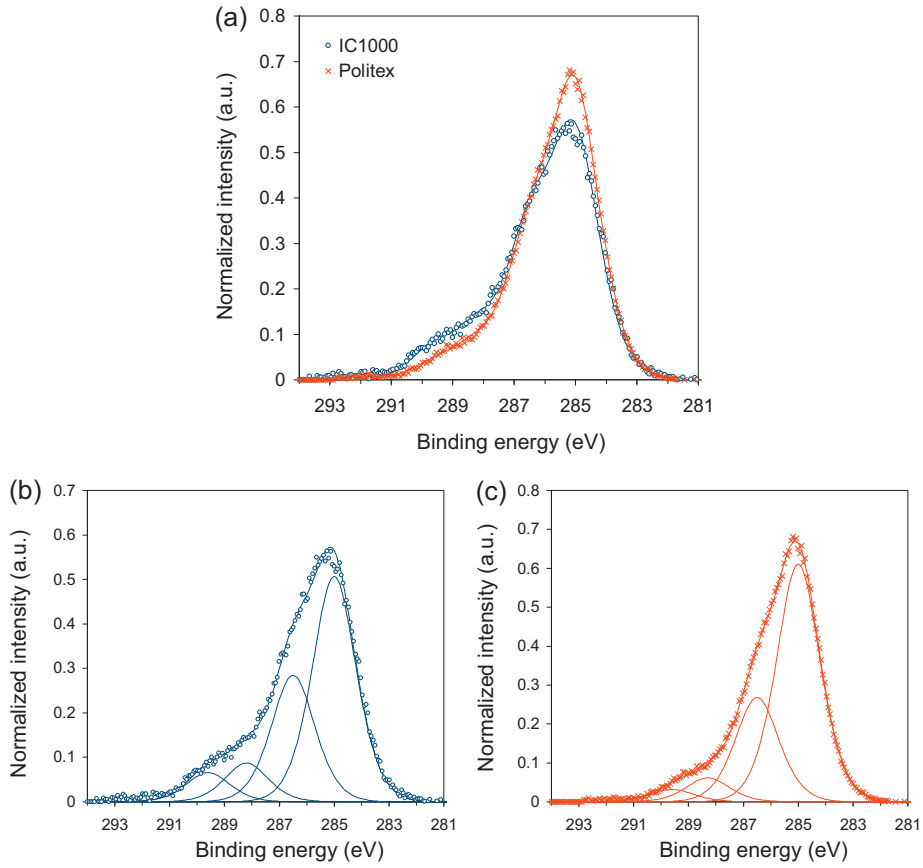

Fig. 5. (a) The area normalized high resolution C 1s XPS spectra of the two pads; (b) subpeaks for the IC1000 pad; and (c) subpeaks for the Politex pad.

polyurethane pad material, or due to pad contamination with silica abrasives that are ubiquitous in a CMP laboratory.

The surface composition of the pad could be significantly different from that in the bulk because of the tendency of the low surface energy non-polar groups to migrate to the surface and the high surface energy polar groups to be buried below the surface. The extent of such a surface reconstruction is determined by the glass transition temperature and crystallinity of the polymer, both of which affect the mobility of the polymer segments. Bulk composition (data not shown) of Cl was, in fact, higher in the Politex pad than in IC1000 pad (0.1 vs 0.03 atomic ratio, normalized based on carbon atoms). Migration of the polar (high surface energy) C–Cl groups into the interior of the pad is more likely in the case of the softer Politex pad than in the harder IC1000 pad. Hence, the surface concentration of Cl is lower in Politex than in IC1000.

Fig. 5a shows the area normalized high resolution C 1s XPS spectra of the two pads. The spectra were resolved into sub-peaks using a series of Gaussian-Lorentzian curves and a Tougaard background (cf. Fig. 5b and c). The peak assignments and the relative areas (number fractions of carbon atoms of a particular type) in the two pads are summarized in Table 2 below. The higher urethane content of IC1000 is consistent with the hardness of this pad. The surface of IC1000 also contains more of the ester [7], amide, and urea linkages that are prone to hydrolysis [22].

Table 2
Peak assignments and the relative areas (number fractions of carbon atoms of a particular type) in the two pads.

Binding energy (eV)	Functional group	IC1000	Politex
285	*C*–H, *C*–C	53.7%	62.8%
286.5	*C*–O, *C*–Cl, *C*–N	30.1%	27.6%
288.3	N–*C*=O (amide), O–*C*=O (ester), N–*C*(=O)–N (urea)	9.2%	6.3%
289.6	O–*C*(=O)–N (urethane)	7.0%	3.3%

3.4. PDADMAC binding differences between IC1000 pad and Politex pad

Based on XPS analysis of the surfaces of the pads, differences in the extent and strength of adsorption of PDADMAC can be attributed to the presence of different amounts of hydrolyzable groups at the surfaces of the two pads. Note that the ester and amide groups are readily prone to hydrolysis [22–24]. Lu et al. [7] have also discussed the hydrolysis of C(=O)–O–C in polyurethane pads. The formation of carboxylate ions due to hydrolysis could be a reason for the negative charges on the pad surfaces. Because the surface concentrations of the hydrolysable groups are higher in the IC1000 pad (cf. Table 2), the anion density and the extent and the strength of PDADMAC adsorption is expected to be higher for IC1000 than Politex.

3.5. Zeta potential data of the pads

Fig. 6 shows the zeta potential data of both pads in the absence and presence of 250 ppm PDADMAC. Other researchers have determined the zeta potentials of the IC1000 and Politex pads [25,26], but the influence of PDADMAC polymer on the pad surface charge has not been reported. In the absence of any additive, the IEP of IC1000 pad is about 3.2 while that of the Politex pad is higher (about 4.2). These results are in agreement with a recent study by Sides et al. [26] who also measured the zeta potentials of both IC1000 and Politex pads using ZetaSpin and observed that the IEP of the flat Politex pad (about 4) is higher than that of the IC1000 pad (about 3).

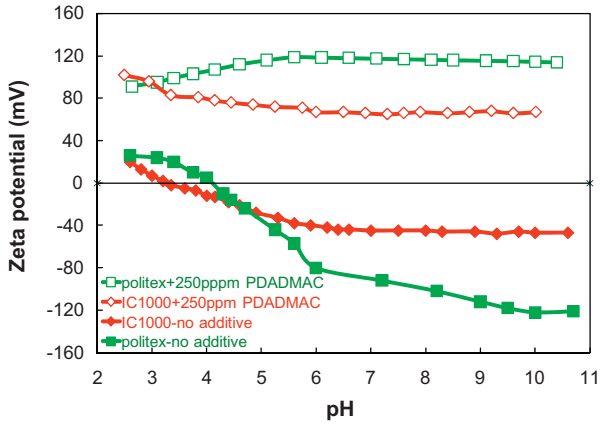

Fig. 6. Zp data of IC1000 and Politex pads in the presence of 0.001 M KCl electrolyte solutions with and without 250 ppm PDADMAC.

They also noticed lower negative zeta potentials on a customized flat Politex pad than those on the original grooved pad, suggesting that creating a flat surface is critical for accurate zeta potential measurements.

Upon the addition of PDADMAC (250 ppm), the pads became positively charged over the entire pH range of the experiment (2.5–10.5), evidently due to adsorption of the cationic polymer on the pad surfaces. The zeta potential of the Politex pad, which was initially immersed and stirred in a PDADMAC solution at pH 10, measured in the presence of only 0.001 M KCl solution is also positive, similar to that measured in the presence of the PDADMAC solution. These zeta potential results seem to indicate that the concentration of adsorbed PDADMAC is higher on the Politex surface than on the IC1000 surface. However, it should be noted that the higher zeta potential values for Politex + PDADMAC could simply be an artifact of the textured surface of the Politex pad (which is not accounted for when the streaming potential values are converted to zeta potentials), in spite of our efforts to smoothen it. Also, the elemental composition and XPS data analysis discussed above suggest that PDADMAC is weakly bound to the Politex pad, confirmed by the dye staining results described below.

3.6. *Qualitative study of polymer adsorption on polishing pads*

Eosin Y (2′,4′,5′,7′-tetrabromofluorescein) is used extensively for staining of proteins and estimating their concentrations [27]. The carboxylate group of the dye binds to the cationic groups in amino-acid residues such as lysine, arginine, histidine and tryptophan to form a protein–dye complex [28]. The formation of the protein–dye complex is easily and visually recognized by a change in the color of the solution from yellow to pink [27,28].

Since PDADMAC is a positively charged cationic polymer and consists of hydrophobic sites, it can also bind with eosin Y. Indeed, as shown in Fig. 7, the yellow color of an aqueous solution of 5 ppm eosin Y changed to pink on adding only 2 ppm of PDADMAC, indicating the formation of a polymer–dye complex. In contrast, when pieces of the two pads, Politex and IC1000, were each dipped in an aqueous solution containing 5 ppm of the dye, there was neither a change in the color of the pad nor in the UV–vis absorption (graphs not shown) of the dye solution, suggesting that the dye does not bind to either of the pads.

However, when pieces of the two pads were first dipped in an aqueous solution of 250 ppm of PDADMAC at pH 10, dried, and then immersed in 5 ppm of eosin Y solution, the solution in which Politex pad was dipped turned pink suggesting the release of PDADMAC from the pad into the dye solution. In contrast, the color of the solution in which IC1000 pad was dipped remained yellow. Moreover,

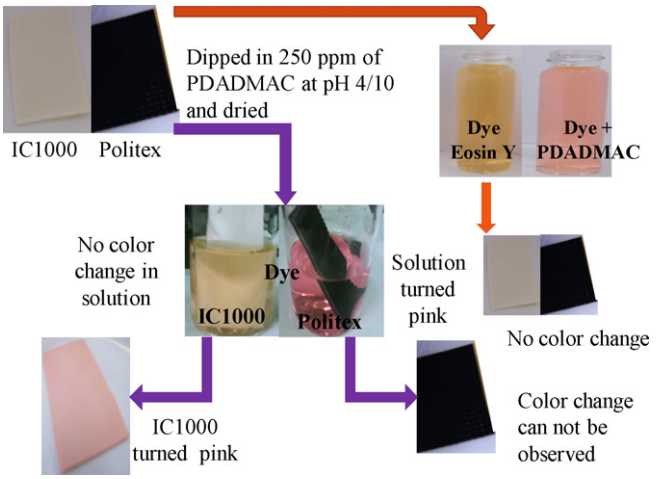

Fig. 7. Experiments to compare the extents of PDADMAC adsorption on IC1000 and Politex pads, using formation of a colored complex with eosin Y dye.

when the IC1000 pad was taken out, the surface appeared pink, suggesting that PDADMAC was indeed present on the IC1000 pad and remained bound to it. With the Politex pad, it was not possible to determine if there was any effect on the color of the pad since the pad is dark. Hence, it could not be determined from this simple experiment if all the PDADMAC was released from the Politex pad. Similar results were obtained when the entire set of experiments was repeated at pH 4.

Further experiments were conducted to confirm the higher adsorption and stronger binding of PDADMAC on IC1000 than on Politex. UV–vis spectra of solutions containing eosin Y (5 ppm) and different concentrations of the polymer, were acquired at a solution pH of 10. In the absence of the polymer, the dye exhibits an absorption peak centered at 516 nm (spectrum a in Fig. 8). Fig. 8 shows the effect of the concentration of added PDADMAC on the intensity of this peak (spectra c–e). The absorption peak shifts to about 525 nm, and a shoulder appears near 495 nm. The new peak and the shoulder can both be associated with the polymer–dye complex as suggested by Hong et al. [28] for protein–dye complexes.

Next, a Politex pad was dipped in an aqueous solution of PDADMAC (250 ppm, pH 10), and dried. This pad was then immersed in the dye solution (5 ppm eosin Y, pH 10) and removed. UV–vis spectrum of the dye solution showed that the maximum in the absorbance was at 524 nm, corresponding to polymer–dye complex

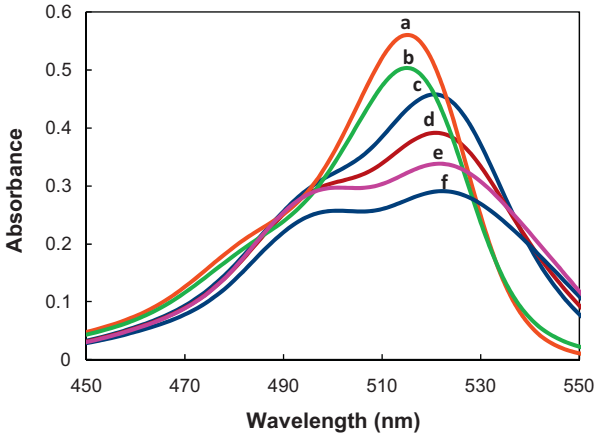

Fig. 8. UV–vis spectra of a 5-ppm aqueous solution of eosin Y at pH 10 (a), and the solution of the dye in the presence of 10, 6, and 4 ppm concentrations of PDADMAC (c, d, and e, respectively). Spectra b and f were obtained from the dye solutions that had contacted PDADMAC-coated IC1000 and Politex pads.

(Fig. 8, spectrum f). Hence, PDADMAC was only weakly adsorbed on Politex, and was released from the pad surface when the pad was immersed in the solution of the dye.

When this procedure was repeated for the IC1000 pad, the absorbance maximum of the dye solution remained at 516 nm (corresponding to the pure dye) (Fig. 8, spectrum b), but with a slight decrease in the peak height, suggesting that some of the dye was consumed in formation of the polymer–dye complex on the pad surface.

These results indicate that PDADMAC adsorbs and is strongly bound to IC1000 pad, and that it also adsorbs on the Politex pad (also suggested by the zeta potential measurements, cf. Fig. 6) but is easily removed from it, indicating a much weaker binding than that in the case of the IC1000 pad.

4. Polishing mechanisms

4.1. Poly-Si removal mechanism in the presence of PDADMAC solutions

Recently, using zeta potential measurements, we suggested that PDADMAC binds to the poly-Si surface and to the IC1000 pad, resulting in polyelectrolyte bridging of the two surfaces [13]. Based on the measured poly-Si RRs, we hypothesized that the bridging interaction is stronger than the polarized and weakened Si–Si bonds of the poly-Si surface. These weaker bonds are ruptured during polishing, resulting in material removal [29]. Earlier, Salmi et al. [30] also noticed a strong PDADMAC-mediated bridging interaction between two cellulosic surfaces, characterized by the pull-off forces determined using atomic force microscope. Several others [31] have extensively discussed the bridging attraction between two solid surfaces with different charge densities in the presence of a polyelectrolyte.

Zeta potential measurements indicate that PDADMAC adsorbs not only on IC1000, but also on Politex (Fig. 6). However, the XPS data (Table 3) and eosin complexation experiments (Fig. 8) indicate that PDADMAC binds with Politex pad only weakly, and is easily solubilized by just dipping in the dye solution. The weaker bonds between the polymer and the Politex pad are easily broken during polishing, which is reflected in the low poly-Si RRs obtained using this pad. It will be useful to measure directly the strength of the bridging forces between PDADMAC molecules, the two pads and the oxide, nitride, and poly-Si surfaces. However, such measurements are complex and lie outside the scope of this paper.

4.2. Effect of PDADMAC-ceria and PDADMAC-silica interaction on poly-Si RRs

Based on zeta potential and thermogravimetry, it was suggested earlier [13] that PDADMAC binds strongly with silica abrasives but only weakly with ceria abrasives. Since PDADMAC-mediated bridging interactions between silica and IC1000 are stronger than those between ceria and IC1000, an addition of silica, but not ceria, enhances poly-Si RR [13]. With the Politex pad, however, there is no enhancement in poly-Si RRs, regardless of whether silica or ceria abrasive is used, because PDADMAC adsorbs only weakly on Politex.

4.3. Oxide and nitride removal mechanism in presence of PDADMAC solutions

Previously, we also suggested that even though PDADMAC forms a strong bond between the IC1000 pad and oxide or nitride surfaces, the adhesive strength of the polymer on oxide and nitride is weaker than the cohesive strength of the oxide and nitride substrates [13]. Hence, during polishing, the polymer–substrate bond is broken easily, resulting in no material removal. Based on the RRs, it appears that the same explanation applies to polishing with Politex pads also.

4.4. Oxide and nitride removal mechanisms using ceria and silica slurries without PDADMAC

From Fig. 2, it is seen that the oxide RRs obtained using ceria slurry at pH 3 differ significantly for the IC1000 and Politex pads. Similarly, a large difference in the RRs is observed at pH 4. These pH values correspond to the isoelectric points of IC1000 and Politex, respectively. Hence, when the pad is changed from IC1000 to Politex, there is a change from electrostatic repulsion to attraction between the ceria abrasives and the pad in this pH interval. Apparently, this is sufficient to influence the RRs. Similarly, the observed decreases in the oxide RR beyond the IEP of ceria (about 8) for both the pads can be due to the shift in the nature of the electrostatic interactions between the ceria and the pads surfaces, from attractive to repulsive. In the case of nitride films, the RRs obtained using the two pads are not significantly different throughout the experimental pH range, presumably because the nitride hydrolysis is the rate controlling step in the removal mechanism [32,33].

Similar changes seen in the nitride RR at pH 4 obtained with silica slurry when the pad was changed from IC1000 to Politex pad can also be a result of the change in the electrostatic interactions among the substrate, silica and the pads.

4.5. Oxide and nitride removal mechanisms using ceria and silica slurries with PDADMAC (250 ppm concentration)

Adding 250 ppm PDADMAC to either ceria- or silica-based slurries, the RRs of both oxide and nitride films were suppressed on both the pads. As discussed earlier [13], this is a result of the adsorption of PDADMAC on both the oxide and nitride surfaces, blocking the contact between the abrasives and the films being polished, and resulting in the suppression of RRs. The pads apparently play no role here.

5. Conclusions

We showed that, while using aqueous solutions of PDADMAC, the poly-Si RRs drop dramatically from about 500 nm/min to <1 nm/min when the polishing pad was changed from an IC1000 pad to a Politex pad. Based on elemental analysis, EDS and XPS data, we hypothesized that the PDADMAC-mediated bridging interaction between the poly-Si surface and the Politex pad is weaker than that between poly-Si and IC1000. Using PDADMAC complex formation with eosin, and UV–vis experiments, we confirmed that PDADMAC interacts only weakly with the Politex pad, but strongly with an IC1000 pad. In the case of IC1000 pad, stronger polycation-mediated bridging interactions with the poly-Si substrate facilitate high RRs by rupturing the underlying Si–Si bonds. In contrast, weaker interaction between PDADMAC and the Politex surface results in no poly-Si removal with this pad.

On adding ceria or silica abrasives to a PDADMAC solution, the poly-Si RRs using the Politex pad were still very low compared to those with the IC1000 pad. In the presence of PDADMAC, the RRs of both oxide and nitride films were suppressed on both pads, presumably due to the stronger substrate Si–O and Si–N bonds (in contrast to the less strong Si–Si bonds in the case of poly-Si) when compared to the strength of the bridging attraction.

Acknowledgements

The authors acknowledge NYSTAR and ARO (Account # W911NF-05-1-0339), Ferro Corporation, Dow Electronic Materials, 3M, and Chris Plunkett for funding, supplying ceria particles, pads, conditioners, and CETR maintenance, respectively. We also thank Professor Sergiy Minko's research group (Clarkson) and Jonathan Shu (CCMR) for help with the zeta potentials measurements and XPS analysis, respectively.

References

[1] L.M. Cook, J.V.H. Roberts, C.W. Jenkins, R.R. Pillai, US Patent 5489233 (1996).; J.V.H. Roberts, US Patent 5,605,760 (1997).; D. Halberg, P. Renteln, US Patent Appl. 0017729 A1 (2009).
[2] R. Bajaj, M. Desai, R. Jairath, M. Stell, R. Tolles, Mat. Res. Soc. Symp. Proc. 337 (1994) 637.
[3] C. Rogers, J. Coppeta, L. Racz, A. Philipossian, F.B. Kaufman, D. Bramono, J. Electronic Mater. 27 (1998) 1082; C.L. Elmufdi, G.P. Muldowney, J. Mater. Res. Symp. Proc. 914 (2006) (Warrendale, PA); S. Armini, C.M. Whelan, M. Moinpour, K. Maex, J. Electrochem. Soc. 156 (2009) H18.
[4] P. Singer, Semicond. Int. 2 (1994) 48; W. O'Mara, Semicond. Int. 7 (1994) 140; D. Rosales-Yeomans, D. DeNardis, L. Borucki, T. Suzuki, A. Philipossian, J. Electrochem. Soc. 155 (2008) H750; D. Rosales-Yeomans, D. DeNardis, L. Borucki, A. Philipossian, J. Electrochem. Soc. 155 (2008) H797.
[5] H. Landis, P. Burke, W. Cote, W. Hill, C. Hoffman, C. Kaanta, C. Koburger, W. lange, M. Leach, S. Luce, Thin Solid Films 220 (1992) 1; Z. Stavreva, D. Zeidler, M. Plotner, K. Drescher, Appl. Surf. Sci. 108 (1997) 39.
[6] T. Murakami, M. Nishio, M. Hamanaka, VMIC Conf. Proc., June 1996.; K. Achuthan, PhD Thesis, Clarkson University, Potsdam, NY, 1998; Y. Moon, D.A. Dornfeld, Proc. Am. Soc. Precision Eng. 18 (1998) 591; W. Li, D.W. Shin, M. Tomozawa, S.P. Murarka, Thin Solid Films 270 (1995) 601; H.-J. Kim, H.-Y. Kim, H.-D. Jeong, MIC Conference, 2000, p. 275; I. Ali, S.R. Roy, G. Shinn, Solid State Technol. 63 (1994); D. Rosales-Yeomans, D. DeNardis, L. Borucki, A. Philipossian, J. Electrochem. Soc. 155 (2008) H812; Y. Sampurno, L. Borucki, Y. Zhuang, S. Misra, K. Holland, D. Boning, A. Philipossian, Thin Solid films 517 (2009) 1719.
[7] H. Lu, B. Fookes, Y. Obeng, S. Machinski, K.A. Richardson, Mater. Charact. 49 (2002) 35.
[8] J.M. Steigerwald, S.P. Murarka, R.J. Gutmann, Chemical–Mechanical Planarization Microelectronic Materials, John Wiley and Sons, New York, 1997.
[9] C. Wang, J. Chang, C.H. Lin, A. Kumar, A. Gehring, J. Cho, A. Majumdar, A. Bryant, Z. Ren, K. Chan, T. Kanarsky, X. Wang, O. Dokumaci, M. Guillorn, M. Khater, Q. Yang, X. Li, M. Naeem, J. Holt, Y. Moon, J. King, J. Yates, Y. Zhang, D. Park, C. Ouyang, W. Haensch, VLSI Tech. Syst. Appl. (2009) 127; J.-P. Colinge, in: J.-P. Colinge (Ed.), FinFETs and Other Multi-Gate Transistors, Springer, New York, 2008, p. 14; A. Kaneko, A. Yagishita, K. Yahashi, T. Kubota, M. Omura, K. Matsuo, I. Mizushima, K. Okano, H. Kawasaki, S. Inaba, I. Izumida, T. Kanemura, N. Aoki, K. Ishimaru, H. Ishiuchi, K. Suguro, K. Eguchi, Y. Tsunashima, IEDM Tech. Digest. (2005) 844.
[10] M. Krishnan, J.W. Nalaskowski, L.M. Cook, Chem. Rev. 110 (2010) 178; Y. Li (Ed.), Microelectronic Applications of Chemical Mechanical Planarization, Wiley-Interscience, 2007, pp. 345, 664.
[11] K. Mistry, C. Allen, C. Auth, B. Beattie, D. Bergstrom, M. Bost, M. Brazier, M.F. Buehler, A. Cappellani, R. Chau, C.-H. Choi, G. Ding, K. Fischer, T. Ghani, R. Grover, W.S. Han, D. Hanken, M. Hattendorf, J. He, J. Hicks, R. Heussner, D. Ingerly, P. Jain, R. James, L. Jong, S. Joshi, C. Kenyon, K. Kuhn, K. Lee, H. Liu, J. Maiz, B. McIntyre, P. Moon, J. Neirynck, S. Pae, C. Parker, D. Parsons, C. Prasad, L. Pipes, M. Prince, P. Ranade, T. Reynolds, J. Sandford, L. Shifren, J. Sebastian, J. Seiple, D. Simon, S. Sivakumar, P. Smith, C. Thomas, T. Troeger, P. Vandervoorn, S. Williams, K. Zawadski, IEEE International Electron Devices Meeting, Washington, D.C., 2007, p. 247.
[12] R.D. Nasby, J.J. Sniegowski, J.H. Smith, S. Montague, C.C. Barron, W.P. Eaton, P.J. McWhorter, D.L. Hetherington, C.A. Apblett, J.G. Fleming, Proceedings of the Solid-State Sensor and Actuator Workshop, SC, 1996, p. 48; J.J. Sniegowski, S.M. Miller, G.F. LaVigne, M.S. Rodgers, P.J. McWhorter, Proc. Solid-State Sensor and Actuator Workshop, SC, 1996, p. 178; R. Howe, Proc. Transducers '95 (1995) 43; W. Tang, T.-C. Nguyen, R. Howe, Sens. Actuators 20 (1989) 25.
[13] N.K. Penta, P.R. Dandu Veera, S.V. Babu, Langmuir 27 (2011) 3502.
[14] W.-C. Chen, C.-T. Yen, J. Polym. Res. 6 (1999) 197.
[15] P.R. Dandu Veera, S. Peddeti, S.V. Babu, J. Electrochem. Soc. 156 (2009) H936.
[16] P.R. Dandu Veera, B.C. Peethala, S.V. Babu, J. Electrochem. Soc. 157 (2009) H869.
[17] T. Okada, European Pat. App. 2287227 A1 (2009).
[18] S. Khatua, Y.-L. Hsieh, J. Polym. Sci. A: polym. Chem. 35 (1997) 3263.
[19] J. Ramsdell, S. Seal, K.A. Richardson, V. Desai, W.G. Easter, Proc. 198th Electrochem. Soc. 26 (2000) 102.
[20] S. Machinski, K. Richardson, W. Easter, Proc. 198th Electrochem. Soc. 26 (2000) 84.
[21] S. Seal, I. Li, K. Richardson, W. Easter, Mat. Res. Soc. Symp. E (2000).
[22] T.M. Chapman, J. Polym. Sci. Part A: Polym. Chem. 27 (1989) 1993.
[23] D.W. Brown, R.E. Lowry, L.E. Smith, Macromolecules 13 (1980) 248.
[24] C. Hepburn, Polyurethane Elastomers, Applied Science Publishers, London, 1982.
[25] I. Sokolov, Q.K. Ong, H. Shodiev, N. Chechik, D. James, M. Oliver, J. Colloid Interface Sci. 300 (2006) 475; A. Dong, G. Hou, Y. Wang, D. Sun, J. Polym. Sci. Part B: Polym. Phys. 40 (2002) 972; U. Mahajan, M. Bielmann, R.K. Singh, Electrochem. Solid state Lett 2 (1999) 80.
[26] P. Sides, R. Rock, S. Shekar, M. Moinpour, M. Buehler, A. Tregub, D. Hooper, International Conf. on Planarization/CMP Technology, Pheonix, 2010.
[27] M.E. Selsted, H.W. Becker, Anal. Biochem. 155 (1986) 270; F. Lin, W. Fan, G.E. Wise, Anal. Biochem. 196 (1991) 279; A.A. Waheed, P.D. Gupta, Anal. Biochem. 233 (1996) 249; M.S.C. Wang, J.S. Pang, M.E. Selsted, Anal. Biochem. 253 (1997) 225; A.A. Waheed, P.D. Gupta, J. Biochem. Biophys. Methods 42 (2000) 125; D. Gao, Y. Tian, F. Liang, Y. Chen, H. Zhang, A. Yu, J. Luminescence 127 (2007) 515.
[28] H.Y. Hong, G.S. Yoo, J.K. Choi, Anal. Lett. 32 (1999) 2427.
[29] P.R. Veera Dandu, B.C. Peethala, H.P. Amanapu, S.V. Babu, J. Electrochem. Soc. 158 (2011) H763.
[30] J. Salmi, M. Osterberg, P. Stenius, J. Laine, Nord. Pulp Pap. Res. J. 22 (2007) 249.
[31] E. Poptosev, P.M. Claesson, Langmuir 18 (2002) 1184; E. Poptosev, P.M. Claesson, Langmuir 18 (2002) 2590; R. Meszaros, I. Varga, T. Gilanyi, Langmuir 18 (2002) 6164; R. Meszaros, I. Varga, T. Gilanyi, Langmuir 20 (2004) 5026.
[32] Y.Z. Hu, R.J. Gutmann, T.P. Chow, J. Electrochem. Soc. 145 (1998) 3919.
[33] E. Laarz, B.V. Zhmud, L. Bergstrom, J. Am. Ceram. Soc. 83 (2000) 2394.